Energy dissipation unveils atomic displacement in the noncontact atomic force microscopy imaging of Si(111)-(7 × 7)

Toyoko Arai,[1] Ryo Inamura,[1] Daiki Kura,[1] and Masahiko Tomitori[2]
[1]*Natural Science and Technology, Kanazawa University, Kanazawa, Ishikawa 920-1192, Japan*
[2]*School of Materials Science, Japan Advanced Institute of Science and Technology, Nomi, Ishikawa 923-1292, Japan*

(Received 28 June 2017; revised manuscript received 6 February 2018; published 19 March 2018)

The kinetic energy of the oscillating cantilever of noncontact atomic force microscopy (nc-AFM) at room temperature was considerably dissipated over regions between a Si adatom and its neighboring rest atom for Si(111)-(7 × 7) in close proximity to a Si tip on the cantilever. However, nc-AFM topographic images showed no atomic features over those regions, which were the hollow sites of the (7 × 7). This energy dissipation likely originated from displacement of Si adatoms with respect to the tip over the hollow sites, leading to a lateral shift of the adatoms toward the rest atom. This interaction led to hysteresis over each cantilever oscillation cycle; when the tip was retracted, the Si adatom likely returned to its original position. To confirm the atomic processes involved in the force interactions through Si dangling bonds, the Si(111)-(7 × 7) surface was partly terminated with atomic hydrogen (H) and examined by nc-AFM. When the Si adatoms and/or the rest atoms were terminated with H, the hollow sites were not bright (less dissipation) in images of the energy dissipation channels by nc-AFM. The hollow sites acted as metastable sites for Si adatoms in surface diffusion and atom manipulation; thus, the dissipation energy which is saturated on the tip likely corresponds to the difference in the potential energy between the hollow site and the Si adatom site. In this study, we demonstrated the ability of dissipation channels of nc-AFM to enable visualization of the dynamics of atoms and molecules on surfaces, which cannot be revealed by nc-AFM topographic images alone.

DOI: 10.1103/PhysRevB.97.115428

I. INTRODUCTION

Noncontact atomic force microscopy (nc-AFM), a type of scanning probe microscopy, has demonstrated excellent capabilities with high force sensitivity between a tip and sample to obtain atom-resolved images of a variety of material surfaces [1–4]. In addition, because the tip-sample separation distance is precisely regulated by the force between the tip and the sample, nanoscale electronic and mechanical properties can be evaluated by measuring force-distance curves, tunneling current, and energy dissipation simultaneously [5–7].

The measurement of energy dissipation, corresponding to a loss of mechanical energy to oscillate an AFM cantilever at a constant amplitude, has been used to examine adhesive atomic processes [8,9], friction forces [10,11], tip-sample atomic configurations [12,13], and Joule heat dissipation [14]. Therein, the conservative forces and nonconservative (dissipative) forces between the tip and sample are apparently separated by in-phase and 90° out-of-phase detections of a phase-locked loop with respect to the cantilever oscillation with a high quality (Q) value [15]. For instance, dissipation images of Si(001)-(2 × 1) clarified that Si dimers adhesively flip-flop as the tip approaches [16]. Interestingly, the nc-AFM and dissipation images of Si(111)-(7 × 7) depicted subsurface atoms, including the backbonds of Si adatoms [17], and clarified the atomic-scale mechanical stiffness of graphene on Pt [18]. However, the interpretation of atomic contrast in dissipation images is still controversial; artifacts often appear in images because of cross talk with the tip tracing of atomic corrugations [19–21] and measurement electronics based on multiple feedback circuits [22,23]. Moreover, the dissipation is sensitive to tip conditions [17,24]. It would be highly desirable to clarify the present of true physical anomalies in the atomic contrast of dissipation images.

Here, we report atomic-scale imaging of Si(111)-(7 × 7) using the dissipation channel of nc-AFM. When a Si tip approaches the sample, the dissipation images depict atomic-featured brighter (dissipative) contrast, not over the Si adatoms, but at hollow sites that are surrounded by surface atoms with dangling bonds in the dimer-adatom stacking-fault (DAS) structure of Si(111)-(7 × 7) [25]. The potential of the dissipation channel is demonstrated for atomic-scale exploration of mechanically dynamic atomic processes such as surface diffusion, abrasion, and manipulation.

II. EXPERIMENTAL

We used a custom-made room-temperature ultrahigh vacuum (UHV, 1×10^{-11}Torr) AFM setup with a Si piezoresistive cantilever with a [001]-oriented Si tip (Veeco) [26]. By passing a direct ∼mA current into a piezoresistor of ∼2kΩ of the cantilever, the cantilever including the tip was cleaned by heating up to 600 °C in the UHV chamber [27,28], leading to a high Q of the cantilever (in the range of 40 000 to 100 000). The nc-AFM (topographic) images were acquired in constant resonant frequency shift (Δf) or constant tip-height modes at a constant oscillation amplitude (A) of the cantilever. In the constant tip-height mode, the average tip-sample separation was kept constant with a weak feedback. The dissipation signal was acquired by measuring the change in the input signal to a dither piezo to oscillate the cantilever at a constant

A at its resonant frequency. Dissipation and time-averaged tunneling-current $\langle I_t \rangle$ images were simultaneously observed with nc-AFM images, which were processed by the WSXM software [29].

The samples were n- and p-type Si(111) rectangular single crystals that were cleaned by flashing at 1200 °C under an UHV to cause (7 × 7) reconstruction [30]. The Si(111)-(7 × 7) surface was examined by nc-AFM. Subsequently, the sample was again flashed, and some of its dangling bonds were terminated with atomic hydrogen (H) at a substrate temperature of 300 °C. The H was generated by cracking of H_2 gas with a tungsten filament at 1500 °C.

III. RESULTS AND DISCUSSION

A. Atomic-scale dissipation increase over noncentered hollow sites of Si(111)-(7 × 7)

Figures 1(a)–1(c) show nc-AFM, $\langle I_t \rangle$, and dissipation images, respectively, of Si(111)-(7 × 7) simultaneously obtained in constant Δf mode. The bright circular regions in Figs. 1(a) and 1(b) correspond to the Si adatoms in the DAS structure [Fig. 1(d)], similar to those in Refs. [2] and [24]. The dissipation image in Fig. 1(c) shows prominent atomic-scale contrast, distinct from those in Figs. 1(a) and 1(b). The distinct bright regions have elongated, lobelike shapes, where the dissipation increased by ∼0.15 eV per cycle of the cantilever oscillation with respect to the values over the Si adatoms and other regions [Fig. 1(c)]. The center of the distinct bright region was at the hexagonal hollow site, indicated by orange ovals in Fig. 1(d), and diagonally surrounded by a Si rest atom and Si adatom, each with a dangling bond. The dissipation over the faulted half-unit cell of (7 × 7) reconstruction was slightly larger than that over the unfaulted half-unit cell. It is noted that the hexagonal hollow site at the center of a triangle of the half-unit cell was dark and was not surrounded by a Si rest atom and Si adatom; hereinafter, it is referred to as the centered hollow site, while the hollow site surrounded by a rest atom and adatom is referred to as the noncentered hollow site. Notably, distinct bright regions were found at a rate of more than 50% with the use of clean Si tips providing stable atomic contrast in the nc-AFM topographic images.

Importantly, the atomic contrast of the dissipation image [Fig. 1(c)] was not the inverted contrast of the nc-AFM topographic image [Fig. 1(a)]. Dissipation images frequently appear as inverted images of the topography [19–21], possibly induced by cross talk of the tip motion tracing the surface corrugation. In Fig. 1, although the tip heights over the noncentered hollow sites were almost the same or slightly higher than those over the centered hollow sites, dimer rows, and corner holes of Si(111)-(7 × 7), we found the prominent increase in dissipation over only the noncentered hollow sites.

To closely examine dependence of dissipation on the tip-sample separation, we imaged the surface in constant tip-height mode. Figure 2 shows the images captured sequentially at three different tip-sample separations. At $\Delta f = -35$ Hz (the tip farthest in Fig. 2), the atomic contrasts in Δf, $\langle I_t \rangle$, and dissipation images exhibited common features [Fig. 2(a)]: the regions over the adatoms were brighter. At this tip-sample separation, the tip apex atom primarily interacted with the Si adatoms, which protruded the most from the Si(111)-(7 × 7) surface. Next, at $\Delta f = -39$ Hz [Fig. 2(b)], the tip approached the surface closer by 15 pm, as evaluated from the Δf-distance curve over a corner hole (not shown here). The contrast in the Δf and $\langle I_t \rangle$ images in Fig. 2(b) did not change much compared with that in Fig. 2(a). However, the dissipation image in Fig. 2(b) exhibited additional small bright spots over the noncentered hollow sites. When the tip approached 70 pm from the height in Fig. 2(b), the dissipation spots over the noncentered hollow sites became noticeably brighter [Fig. 2(c)], and their features resembled those in Fig. 1(c). The dissipation dependence on the tip-sample separation indicates that the dissipation over the noncentered hollow sites is not caused by cross talk with the tip motion.

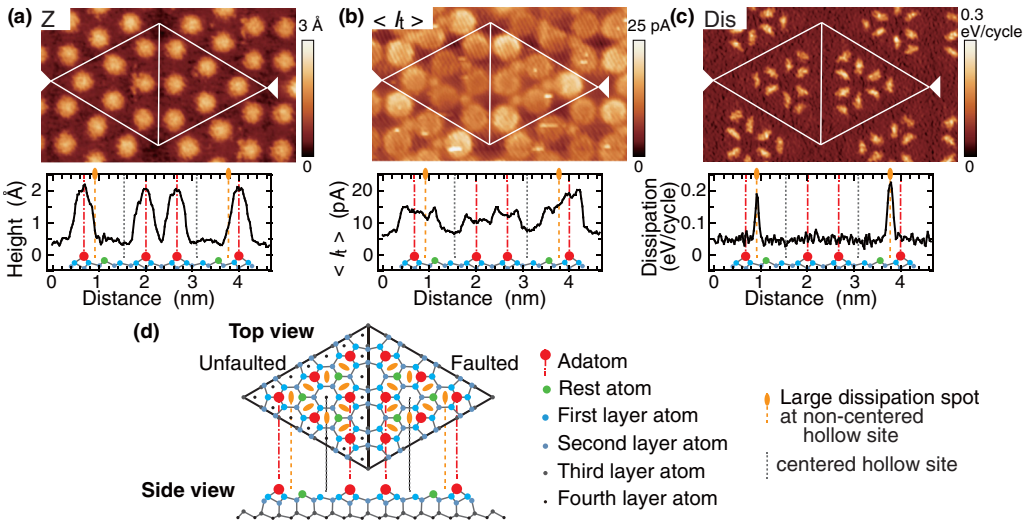

FIG. 1. (a) nc-AFM image of n-type Si(111)-(7 × 7) in constant Δf mode obtained simultaneously with (b) $\langle I_t \rangle$ and (c) dissipation images, at $\Delta f_{set} = -42$ Hz, $V_{sample} = -0.37$ V [contact potential difference (CPD) canceled], with a cantilever of $f_0 = 218$ kHz, $Q = 92300$, spring constant $k = 14.7$ N/m, and $A = 16.3$ nm. Image area: 5.6 × 3.4 nm^2. The cross-sectional profile between the two arrow heads is shown at the bottom of each image. (d) Top and side views of the Si(111)-(7 × 7) model. Orange ovals show the distinct dissipation regions.

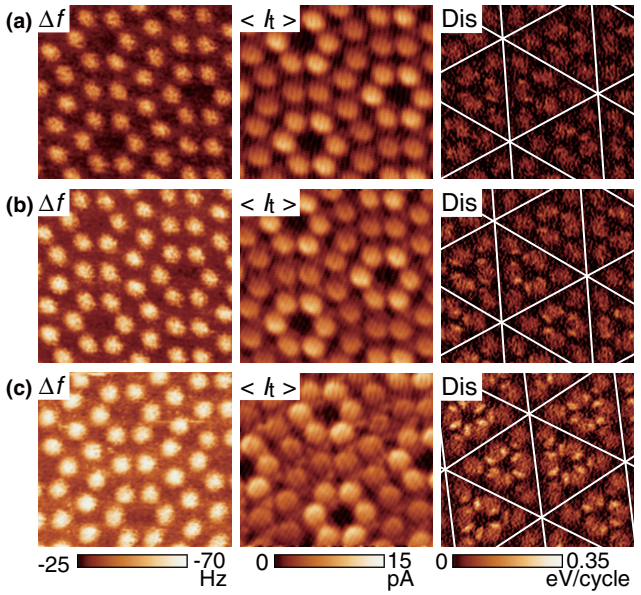

FIG. 2. Simultaneously obtained images of Δf, $\langle I_t \rangle$, and dissipation of Si(111)-(7 × 7) in constant tip-height mode at f_{set} of (a) −35 Hz, (b) −39 Hz [15 pm closer than in (a)], and (c) −47 Hz [70 pm closer than in (b)] at $V_{sample} = +50$ mV for CPD = −290 mV, with a cantilever of $f_0 = 199$ kHz, $Q = 41900$, $k = 8.5$ N/m, and $A = 19$ nm. Image area: 5.0 × 4.5 nm^2.

Regarding the energy dissipation, it is most likely that the atomic configurations of the tip and sample change as the tip approaches and retracts, accompanied by a hysteresis loop in the force-distance curve [8,9]. Majzik *et al.* reported that the dissipation over Si adatom sites, which increased with decreasing tip-sample distance, was attributed to adhesive hysteresis [24]. Intricate atomic dynamic processes causing the hysteresis loops could occur between the Si tip, rest atoms, and adatoms with dangling bonds around the noncentered hollow sites. During its approach and retraction, the tip experiences a force potential with quasiequilibrium minima imparted by potential barriers, where the potential curve changes with the tip-sample separation. Kantorovich and Trevethan [9] calculated that the event of crossing the barriers for the tip-sample system thermodynamically fluctuates during tip oscillation, resulting in an inconstant hysteresis loop for each oscillation cycle.

We measured Δf-distance and dissipation-distance curves over the corner adatom and its neighboring noncentered hollow site in the faulted half-unit cell. Figure 3 contains a plot of the contribution from the short-range forces f_{SR}; the contribution from the long-range forces was subtracted from Δf [31]. The Δf_{SR}-distance curves exhibited exponential decays at distances farther than 1.5 Å over the adatom and 0.9 Å over the hollow site with respective decay lengths of 120 and 160 pm; the decay length over the adatom was close to that reported in Ref. [32]. The dissipation increased with decreasing distance less than 1.5 Å to saturate at 0.07 eV/cycle over the adatom, and less than 0.9 Å to saturate at 0.35 eV/cycle over the hollow site. The small increase in dissipation over the adatom site was likely caused by the vertical upward displacement of the Si adatom during tip retraction through the elongated

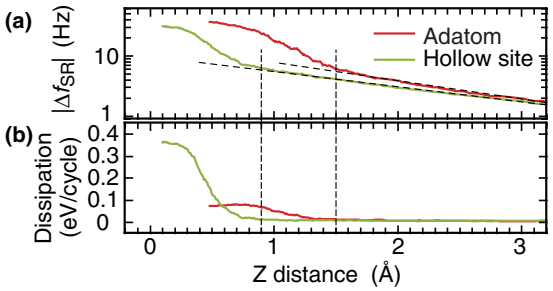

FIG. 3. (a) Logarithmic-scale frequency shift caused by short-range forces (Δf_{SR})-distance curves, and (b) dissipation-distance curves at the corner adatom (red), and its neighboring noncentered hollow site (green) at $V_{sample} = -0.39$ V to cancel CPD, with a cantilever of $f_0 = 218$ kHz, $Q = 92\,000$, $k = 14.7$ N/m, and $A = 12.2$ nm. Distance = 0 is the closest distance in the measured curves. The sample was p-type Si(111)-(7 × 7).

bond with the Si tip in an adhesive hysteresis loop [24]. The large increase in dissipation over the hollow site seemed to be related to more intricate changes in the atomic configuration. At the distances where the dissipation increased, the Δf_{SR} value became slightly larger, deviating from the exponential behavior at distant separations. This deviation indicates an abrupt increase in attractive forces during the tip approach in the hysteresis loop, whereas the Δf_{SR} value corresponds to the force weight-averaged over the loop, in phase with the cantilever oscillation [9].

B. Hydrogen termination of Si dangling bonds clarifying their roles in dissipation

To clarify the role of the dangling bonds in dissipation, we partially terminated the Si(111)-(7 × 7) surface with H, resulting in chemical inactivation of some of the dangling bonds. The atomic contrast in the nc-AFM image [Fig. 4(a)] seemed similar to that of the nonterminated surface, as shown in Fig. 1(a), except for one darker Si adatom site, which was likely terminated with H, because the force between the tip and the H-terminated adatom was weakened. Conversely, in the $\langle I_t \rangle$ image [Fig. 4(b)], some adatom sites became noticeably brighter. Changes in I_t caused by H termination have been detected by scanning tunneling microscopy (STM) [33] and theoretical calculations [34]; initially, the Si rest atoms are preferentially terminated with H. Although rest atoms cannot usually be imaged by STM, the H-terminated rest atoms alter the electronic states of the neighboring Si adatoms, resulting in the Si adatoms appearing brighter in the STM images. The $\langle I_t \rangle$ image [Fig. 4(b)], roughly corresponding to the STM image, implies that the Si rest atoms next to the bright adatom sites are terminated with H. The images in Fig. 4 were simultaneously observed in constant Δf mode so that the tip retracted over the nonterminated Si adatoms and approached the H-terminated Si adatom and the rest atoms. Consequently, although the density of states over the H-terminated Si adatom and rest atoms decreased, the tunneling current increased with decreasing tip-sample distance, resulting in the observed current contrast [Fig. 4(b)]. Figure 4(d) shows a model for the H-terminated sites, estimated from Figs. 4(a) and 4(b), where orange ovals

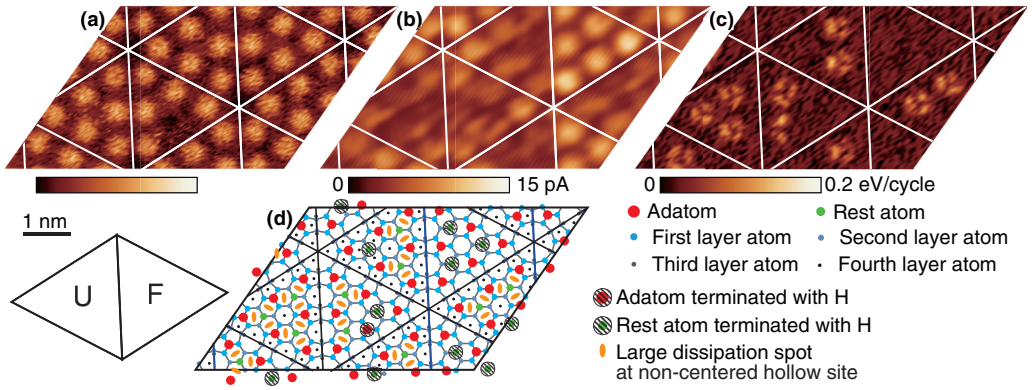

FIG. 4. (a) nc-AFM image of partially H-terminated p-type Si(111)-(7 × 7) in constant Δf mode obtained simultaneously with (b) $\langle I_t \rangle$, and (c) dissipation images at $\Delta f_{set} = -30$ Hz, $V_{sample} = -0.60$ V for CPD $= -0.31$V, with a cantilever of $f_0 = 199$ kHz, $Q = 47\,800$, $k = 8.5$ N/m, and $A = 19$ nm. Image area was 6.0×3.5 nm^2 with drift compensation sheared at 35°. White meshes show the unit cells. (d) Atomistic model of H-terminated Si(111)-(7 × 7). Estimated H-terminated sites are hatched.

denote the large dissipation regions in Fig. 4(c) (a detailed H-termination model is illustrated in Fig. S1 of Supplemental Material [35]). Some distinct bright (large dissipation) regions over the noncentered hollow sites in the dissipation image were lost, which coincided with the hollow sites next to H-terminated rest atoms and/or H-terminated adatom. This result indicates that the dangling bonds of the rest atom and adatom around the hollow site affect the dissipation. Note that a H-terminated Si tip did not provide distinct bright contrast over the hollow sites in our experiments, indicating that the dangling bond of the tip also plays a crucial role in dissipation.

The hollow sites play an important role in the surface diffusion of adatoms on Si(111); Si adatoms move back and forth between neighboring hollow sites with an activation energy of 0.3–0.8 eV [36]. Adatom diffusion would be initiated by breakage of one of the three backbonds between the adatom and underlying layer, which is on the opposite side of the destination hollow site. This effect reflects the rotational motion of a Si tetrahedron, at the center of which is the adatom; however, no Si atom is on the top of the tetrahedron, around the axis line connecting the bottom ends of the remaining two backbonds. The adatom position shifts while a new backbond is being formed with the Si rest atom next to the destination hollow site.

C. Dissipation mechanism feasible for the atomic-scale contrast

Assuming that the tip has a Si atom with a dangling bond at its apex, which is stably localized by the heat treatment under UHV, we propose the following intuitive model for the dissipation. When the tip approaches over the Si adatom, because the adatom is bound to the surface through three backbonds, the Si adatom cannot easily move laterally on the surface. The adatom might move vertically slightly through the interaction with the tip. When the tip approaches the side of adatom from the top (the side facing the neighboring hollow site) [Fig. 5(a)], the dangling bond of the tip interacts with the dangling bond of the Si adatom at a slant, which likely drags the Si adatom toward the hollow site and breaks one backbond; this process is analogous to that of a nail puller working with torque [Fig. 5(b)]. Compared with other Si surface atoms, such as rest atoms, Si adatoms can be more easily manipulated owing to their sp^3 orbitals, which are distorted from those in the bulk diamond structure of Si. As the tip approaches closer to the surface, the distance between the adatom and rest atom next to the hollow site becomes smaller, resulting in the formation of a new backbond between them [Fig. 5(c)]. This process is similar to that of a H_2 molecule dissociatively adsorbing on Si(111)-(7 × 7); when H_2 approaches the hollow site between a Si adatom and Si rest atom, one backbond of the adatom and the bond of the H_2 molecule break through the interaction with the rest atom, resulting in H termination of both the adatom and rest atom, as reported in Ref. [37] through first-principles functional theory calculations.

Our intuitive model is based on the above atomic processes. When the tip approaches, one backbond of the adatom

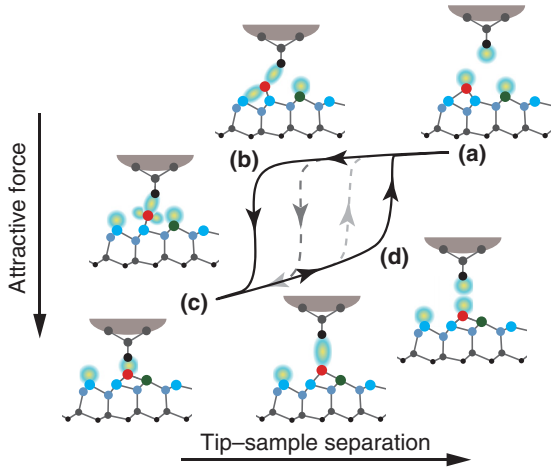

FIG. 5. Model of backbond breaking and formation during a tip approach and retraction cycle with a hysteresis loop in the force-distance curve. The [001]-oriented Si tip is over the noncentered hollow site in (a). The position of the adatom (red) is shifted by the tip approaching in (b), and the backbond is broken, resulting in the alternative atomic configuration with three backbonds in (c). Subsequently, the tip retracting slightly lifts up the adatom, breaks the bond in (d), and finally the adatom returns to its original site thermodynamically. The hysteresis loop in gray shows its thermodynamic fluctuation.

breaks and a bond forms between the adatom and rest atom. Then, the attractive force suddenly increases as a snap-in [Fig. 5(c)]. During retraction, the bond between the adatom and the Si tip atom would be vertically extended, resulted in bond breaking [Fig. 5(d)]. Subsequently, the Si adatom thermodynamically returns to the original adatom site at a stable atomic configuration on Si(111)-(7 × 7), crossing the surface-diffusion barrier, which is lowered by the tip close to the adatom, as evaluated for atom manipulations [38–40]. The observed energy dissipation could originate from this sort of hysteresis loop [8,9]. According to calculations of adatom diffusion [36], the energy difference for the Si adatom between the neighboring hollow sites is approximately 0.4 eV, which is close to the saturated dissipation value of 0.35 eV [Fig. 3] and corresponds to the net work done by the tip to move the adatom from the original adatom site to the hollow site. Notably, the tip approaching the other side of the Si adatom would also break the backbond at the side opposite to the approaching tip. However, the process would be elastic with much less dissipation, because the Si surface atom with a dangling bond does not exist on the side where the tip approaches. To verify our model, further theoretical calculations are required.

Notably, in the nc-AFM topographic image [Fig. 1(a)], the bright regions at the adatom sites were circular (see contour map of Fig. 1(a) shown in Fig. S2 of Supplemental Material [35]). The sensitivity of the Δf signal to the change over the noncentered hollow site was insufficient, because the Δf signal contains the terms of long-range interactions between the tip and the sample. Meanwhile, the terms are canceled in the dissipation channel by averaging weighted 90° out of phase through a line integral along the hysteresis loop, resulting in the high sensitivity of the dissipation channel to the dynamic atomic processes with hysteresis.

We also anticipate that the displaced Si adatom over the noncentered hollow site would remain longer at low temperatures, leading to direct observation of the Si atoms over the noncentered hollow sites with low-temperature nc-AFM.

IV. CONCLUSION

We found distinct atomic contrast over noncentered hollow sites in dissipation channel images of Si(111)-(7 × 7). In close proximity, the interaction between the Si tip and Si adatom, which are off-aligned, likely leads to backbond breaking and subsequent bond formation with a Si rest atom, accompanied by the energy dissipation through the hysteresis loop of the force-distance curves. The dissipation channel can provide crucial information for analysis of mechanically dynamic atomic processes involving bond breaking and formation, such as surface atom diffusion, atomic abrasion, and manipulation, which can hide behind atom-resolved nc-AFM and $\langle I_t \rangle$ images.

ACKNOWLEDGMENTS

This work was supported by the Japanese Society for the Promotion of Science (JSPS) KAKENHI Grants No. 16H02076 and No. 26600098, Kanazawa University SAKIGAKE Project, and partly by Shibuya Science Culture and Sports Foundation.

[1] F. J. Giessibl, Science **267**, 68 (1995).
[2] S. Morita, R. Wiesendanger, and E. Meyer, *Noncontact Atomic Force Microscopy* (Springer-Verlag, Berlin, 2002).
[3] C. Barth, A. S. Foster, C. R. Henry, and A. L. Shluger, Adv. Mater. **23**, 477 (2011).
[4] J. V. Lauritsen and M. Reichling, J. Phys.: Condens. Matter. **22**, 263001 (2010).
[5] S. Morita, F. J. Giessibl, and R. Wiesendanger, *Noncontact Atomic Force Microscopy*, Vol. 2 (Springer-Verlag, Berlin, 2009).
[6] S. Sadewasser and T. Glatzel, *Measuring and Compensating Electrostatic Forces* (Springer-Verlag, Berlin, 2012).
[7] S. Morita, F. J. Giessibl, E. Meyer, and R. Wiesendanger, *Noncontact Atomic Force Microscopy*, Vol. 3 (Springer International Publishing, Switzerland, 2015).
[8] N. Sasaki and M. Tsukada, Jpn. J. Appl. Phys. **39**, L1334 (2000).
[9] L. N. Kantorovich and T. Trevethan, Phys. Rev. Lett. **93**, 236102 (2004).
[10] M. Gauthier and M. Tsukada, Phys. Rev. B **60**, 11716 (1999).
[11] T. Trevethan and L. Kantorovich, Phys. Rev. B **70**, 115411 (2004).
[12] N. Oyabu, P. Pou, Y. Sugimoto, P. Jelínek, M. Abe, S. Morita, R. Pérez, and O. Custance, Phys. Rev. Lett. **96**, 106101 (2006).
[13] G. Langewisch, W. Kaminski, D. A. Braun, R. Moller, H. Fuchs, A. Schirmeisen, and R. Perez, Small **8**, 602 (2012).
[14] W. Denk and D. W. Pohl, Appl. Phys. Lett. **59**, 2171 (1991).
[15] H. Hölscher, B. Gotsmann, W. Allers, U. D. Schwarz, H. Fuchs, and R. Wiesendanger, Phys. Rev. B **64**, 075402 (2001).
[16] J. Bamidele, Y. J. Li, S. Jarvis, Y. Naitoh, Y. Sugawara, and L. Kantorovich, Phys. Chem. Chem. Phys. **14**, 16250 (2012).
[17] D. Sawada, Y. Sugimoto, M. Abe, and S. Morita, Appl. Phys. Express **3**, 116602 (2010).
[18] B. de la Torre, M. Ellner, P. Pou, N. Nicoara, R. Pérez, and J. M. Gómez-Rodríguez, Phys. Rev. Lett. **116**, 245502 (2016).
[19] R. Lüthi, E. Meyer, M. Bammerlin, A. Baratoff, L. Howald, C. Gerber, and H.-J. Güntherodt, Surf. Rev. Lett. **4**, 1025 (1997).
[20] C. Loppacher, R. Bennewitz, O. Pfeiffer, M. Guggisberg, M. Bammerlin, S. Schär, V. Barwich, A. Baratoff, and E. Meyer, Phys. Rev. B **62**, 13674 (2000).
[21] T. Arai and M. Tomitori, Appl. Phys. A: Mater. Sci. Process. **72**, S51 (2001).
[22] M. Gauthier, R. Pérez, T. Arai, M. Tomitori, and M. Tsukada, Phys. Rev. Lett. **89**, 146104 (2002).
[23] A. Labuda, Y. Miyahara, L. Cockins, and P. H. Grütter, Phys. Rev. B **84**, 125433 (2011).
[24] Z. Majzik, M. Setvín, A. Bettac, A. Feltz, V. Cháb, and P. Jelínek, Beilstein J. Nanotechnol. **3**, 249 (2012).
[25] K. Takayanagi, Y. Tanishiro, M. Takahashi, and S. Takahashi, J. Vac. Sci. Technol. A **3**, 1502 (1985).
[26] T. Arai and M. Tomitori, Appl. Surf. Sci. **157**, 207 (2000).
[27] T. Arai and M. Tomitori, Jpn. J. Appl. Phys., Part 1 **36**, 3855 (1997).

[28] M. Tomitori and T. Arai, Appl. Surf. Sci. **140**, 432 (1999).
[29] I. Horcas, R. Fernández, J. M. Gómez-Rodríguez, J. Colchero, J. Gómez-Herrero, and A. M. Baro, Rev. Sci. Instrum. **78**, 013705 (2007).
[30] T. Arai and M. Tomitori, Appl. Phys. Lett. **86**, 073110 (2005).
[31] M. A. Lantz, H. J. Hug, R. Hoffmann, P. J. A. van Schendel, P. Kappenberger, S. Martin, A. Baratoff, and H. J. Güntherodt, Science **291**, 2580 (2001).
[32] Y. Sugimoto, M. Ondracek, M. Abe, P. Pou, S. Morita, R. Pérez, F. Flores, and P. Jelínek, Phys. Rev. Lett. **111**, 106803 (2013).
[33] I. C. Razado, H. M. Zhang, R. I. G. Uhrberg, and G. V. Hansson, Phys. Rev. B **71**, 235411 (2005).
[34] H. Lim, K. Cho, I. I. Park, J. D. Joannopoulos, and E. Kaxiras, Phys. Rev. B **52**, 17231 (1995).
[35] See Supplemental Material at http://link.aps.org/supplemental/10.1103/PhysRevB.97.115428 for a model of disappearance of the distinct bright spots over the non-centered hollow sites for a partially H-terminated Si(111)-(7×7) surface [Fig. S1], and the contour map of the nc-AFM topographic image in Fig. 1(a) [Fig. S2].
[36] T. Hoshino, M. Hata, and M. Tsuda, Surf. Sci. **481**, 205 (2001).
[37] K. Cho, E. Kaxiras, and J. D. Joannopoulos, Phys. Rev. Lett. **79**, 5078 (1997).
[38] Y. Sugimoto, P. Jelinek, P. Pou, M. Abe, S. Morita, R. Perez, and O. Custance, Phys. Rev. Lett. **98**, 106104 (2007).
[39] Y. Sugimoto, K. Miki, M. Abe, and S. Morita, Phys. Rev. B **78**, 205305 (2008).
[40] B. Enkhtaivan and A. Oshiyama, Phys. Rev. B **95**, 035309 (2017).